Longitudinal Modeling of Multi-modal Image Contrast Reveals Patterns of Early Brain Growth

Avantika Vardhan[1], James Fishbaugh[2(✉)], Clement Vachet[1], and Guido Gerig[2]

[1] Scientific Computing and Imaging Institute, University of Utah,
Salt Lake City, UT, USA
[2] Tandon School of Engineering, New York University, New York, NY, USA
james.fishbaugh@nyu.edu

Abstract. The brain undergoes rapid development during early childhood as a series of biophysical and chemical processes occur, which can be observed in magnetic resonance (MR) images as a change over time of white matter intensity relative to gray matter. Such a contrast change manifests in specific patterns in different imaging modalities, suggesting that brain maturation is encoded by appearance changes in multi-modal MRI. In this paper, we explore the patterns of early brain growth encoded by multi-modal contrast changes in a longitudinal study of children. For a given modality, contrast is measured by comparing histograms of intensity distributions between white and gray matter. Multivariate non-linear mixed effects (NLME) modeling provides subject-specific as well as population growth trajectories which accounts for contrast from multiple modalities. The multivariate NLME procedure and resulting non-linear contrast functions enable the study of maturation in various regions of interest. Our analysis of several brain regions in a study of 70 healthy children reveals a posterior to anterior pattern of timing of maturation in the major lobes of the cerebral cortex, with posterior regions maturing earlier than anterior regions. Furthermore, we find significant differences between maturation rates between males and females.

1   Introduction

Appearance in MR scans serves as a noninvasive indicator of underlying tissue composition and biochemistry. Brain MR scans clearly show variations in tissue appearance as a result of neurological changes. These appearance variations have been tracked to provide insights into neurological disease progression, aging, and brain development [1]. During early stages of infant brain development, crucial biophysical and chemical changes, such as myelination, manifest as rapid variations in white matter (WM) intensity [2]. These changes in WM intensity are commonly observed in T1W and T2W MR scans. The analysis of WM intensity

changes therefore serves as the basis for many quantitative neurodevelopmental studies of MR appearance [1,3]. However, using WM intensity measurements alone proves unstable, as voxels in T1W and T2W MR scans show intensity values that are highly variable with respect to several external factors, including scanner settings and scanning conditions [4].

This problem can be overcome by using advanced, quantitative MR scanning techniques such as MWF (Myelin Water Fraction) [5], and quantitative T2 maps. However, the acquisition of new images does not alleviate the need to analyze large retrospective studies consisting of mainly T1W and T2W MR scans. An alternative is to utilize normalization schemes to standardize MR intensity values [3,6], however, these procedures are often complex and unsuitable for infant brain scans. To reduce dependence on normalization procedures while ensuring invariance in appearance computation to external conditions of scan, this work adopts an inter-tissue contrast measure.

The contrast measure used quantifies relative intensity variations between white and gray matter tissue classes using the Hellinger distance (HD) between their intensity distributions, ensuring invariance to affine transformations of underlying intensities due to properties of HD [7]. Further, spatiotemporal analysis of the contrast change over time using nonlinear mixed-effects (NLME) modeling techniques results in quantification of regional appearance change parameters from which inferences related to brain maturation can be drawn. Multivariate and multilevel NLME modeling schemes also enable characterization of inter-modality and inter-population differences in appearance change trajectories.

The primary contribution of this paper lies in application of the above methodology to an infant brain imaging dataset consisting of repeated scans from 70 healthy subjects obtained across 3 time points between birth and 2 years of age. As a result of longitudinal modeling of appearance parameters it is possible to compare delay in developmental trajectories across brain regions, modalities, and population groups. Inferences from analysis of sex differences using a multilevel longitudinal model show delay in appearance change between male and female groups, demonstrating the potential clinical value of the method. To the best of our knowledge, this is the first large-scale study of appearance change during infant brain development in terms of inter-tissue contrast.

2   Methods

Spatiotemporal modeling of inter-tissue contrast involves an optimized 4D longitudinal pipeline to ensure accurate generation of tissue segmentations and brain parcellations. These segmentation and parcellation maps are then used to create intensity distributions for WM and GM tissue classes specific to each major cortical region. The contrast measure for each cortical region is then computed in terms of the overlap between the WM and GM intensity distribution belonging to that region. Such regional contrast measures are also obtained for each modality. Finally, spatiotemporal growth patterns in the resulting multi-modal contrast data are modeled via the non-linear mixed effects (NLME) method.

Parameters of interest are extracted and analyzed from the NLME fit in order to characterize spatiotemporal trajectories of contrast change.

Preprocessing: It is well established that early gyrification of the brain ensures consistent neuroanatomy in infant brains during early brain development, despite large volumteric changes [8]. The 4D longitudinal pipeline used in this work, which consists of co-registration, tissue segmentation, and regional parcellation of the brain, is optimized to utilize this characteristic of subject-specific neuroanatomical consistency across time.

Inter-subject registration is performed using the ANTS framework with a choice of cross-correlation as the metric for diffeomorphic mappings. Inter-subject registration was then performed by computing a population atlas based on the deformation of latest time point scans using the large deformation framework [9], leveraging the high inter-tissue contrast seen in later time point scans.

Segmentation of the multimodal brain scans into major tissue classes was done using an expectation maximization framework which utilized probabilistic priors [10]. The effectiveness of a longitudinal segmentation framework, which uses high-contrast, late-time point image segmentations to enforce a prior on low-contrast, earlier time point images has already been established [8]. The latest time point uses probabilistic priors from an existing population atlas, and in turn provides priors for earlier time points.

To perform parcellation of the brain into major cortical regions, a parcellation atlas from a previous large-scale neuroimaging study is co-registered with the latest time point image from the series of infant scans. The atlas is co-registered with scans from previous time points by using the intra-subject deformations computed earlier. As a result of this pre-processing pipeline, each voxel in the multimodal set of m brain scans at a time point t_j and belonging to subject i is given two labels: (a) a tissue-class label c_k (based on segmentation), and (b) a cortical-region label R_l (from parcellation).

Intensity distributions: Let I_{i,t_j}^m represent the scan from the i-th subject at time t_j (corresponding to the jth time point) and belonging to modality m. Corresponding to each scan is a label image resulting from tissue segmentation, which assigns every voxel to a tissue class c_k, as well as another label image from parcellation, which assigns every voxel to an anatomical region R_l. Intensity distributions are computed by sampling voxels belonging to the tissue class and region under analysis. For every I_{i,t_j}^m, we use kernel density estimation (KDE) to obtain a smooth and continuous intensity distribution for each tissue class c_k and region R_l.

Consider the intensity distribution for the scan I_{i,t_j}^m defined above. For the modality m scan belong to subject i, acquired at timepoint t_j, the probability of a given intensity Int_q being exhibited by voxels belonging to tissue class c_k and region R_l is computed by

$$P_{i,t_j}^m(Int_q|c_k, R_l) = \frac{1}{nh} \sum_{x \in \{c_k, R_l\}} G\left(\frac{Int_q - Int(I_{i,t_j}^m(x))}{h}\right), \qquad (1)$$

where n denotes the number of voxels $x \in \{c_k, R_l\}$, $int(I_{i,t_j}^m(x))$ is the intensity of image I_{i,t_j}^m at voxel x, and h is the bandwidth of the Gaussian kernel G.

The purpose of converting raw intensity values into a distribution is for comparison of image appearance between scans or between different regions of the same scan, along with removal of any associated shape or volume information. When compared with voxel-wise intensity comparisons, intensity distributions eliminate the need for accurate image co-registration. Using a probability density function for intensity representation also ensures that volumetric information from the contributing region is eliminated.

Quantification of contrast: Measuring relative intensity variations in terms of inter-tissue contrast ensures sensitivity to WM-GM appearance changes resulting from neurodevelopment, while reducing variability due to external factors (eg. scan conditions). Given two probabilistic intensity distributions (WM and GM), the variations between them can be quantified by the overlap between their distributions. Such a measure can capture subtle variations that cannot be effectively measured by summary statistics such as difference in mean intensity.

The measure used in this work to quantify inter-tissue contrast is denoted White-gray Intensity Variation in Infant Development (WIVID). WIVID quantifies inter-tissue contrast between WM and GM by computing the Hellinger Distance between their respective intensity distributions, which captures the divergence between two probabilistic distributions [11]. Therefore, as the inter-tissue contrast between WM and GM increases, this results in a corresponding increase in the WIVID measure. Similarly, a decrease in inter-tissue contrast between WM and GM results in a decrease in the WIVID measure.

Consider the image of modality m belonging to subject i at time t_j, denoted I_{i,t_j}^m. WM and GM intensity distributions for this scan can be computed using Eq. (1), with $c_k = WM$ and $c_k = GM$ for the respective tissue class distributions estimated for a region R_l. The WIVID measure for this region can now be computed in terms of the Hellinger Distance (denoted by HD) as

$$WIVID_{i,m}^{R_l}(t_j) = HD(P_{im}(Int, t_j | c_k = WM, R_l), P_{im}(Int | c_k = GM, R_l)). \quad (2)$$

Longitudinal modeling of multi-modal contrast: We briefly summarize the NLME model [12]. Consider a population of N_{ind} individual subjects indexed by i and the T_{ind} time points of scan are denoted by j. The contrast variable $WIVID_{ij}$ belonging to the ith subject at the jth time point t_{ij}, can be written in terms of the NLME equation as

$$WIVID_{ij} = f(\boldsymbol{\phi}_i, \mathbf{t}_{ij}) + e_{ij}, \quad (3)$$

The mixed effects function used to model the change in the variable is written as f. This function is dependent on the temporal variable t_{ij} as well as the mixed-effect parameter vector $\boldsymbol{\phi}_i$ that is specific to each subject. The error term e_{ij} indicates the i.i.d error following the distribution $e_{ij} \sim N(0, \sigma^2)$. The core component of the NLME model is the mixed effect parameter vector $\boldsymbol{\phi}_i$ which can be written in terms of its fixed and random effects components

$$\boldsymbol{\phi}_i = \boldsymbol{A_i\beta} + \boldsymbol{B_ib_i} \ , \text{ where } \boldsymbol{b_i} \sim N(0, \boldsymbol{\psi}). \tag{4}$$

with fixed and random effects design matrices $\boldsymbol{A_i}$ and $\boldsymbol{B_i}$ for each subject i. The p-vector of fixed effects is given by $\boldsymbol{\beta}$ and the q-vector of random effects is given by $\boldsymbol{b_i}$. The random effects matrix $\boldsymbol{b_i}$ is assumed to be normally distributed with variance-covariance matrix $\boldsymbol{\psi}$ over all subjects.

Non-linear asymptotic growth is modeled by the logistic function

$$f(t) = \frac{\phi_1}{1 + \exp(\frac{\phi_3 - t}{\phi_2})}. \tag{5}$$

with intuitive parameters: ϕ_1 denoting right asymptote, ϕ_2 denoting speed of development, and ϕ_3 is the midpoint (inflection point), denoting delay.

The NLME model in Eq. (3) can then be used to evaluate the logistic function in Eq. (5). Practically, not all parameters have both fixed and random effects components particularly since this might result in an unstable estimate due to an increase in number of variables. In our analysis, ϕ_1 (right asymptote) and ϕ_3 (delay) parameters were modeled with non-zero random effects, while it was assumed that the speed parameter had no random effects component. Note that in this multivariate model, the random effects parameters of all modalities have a joint variance-covariance matrix which accounts for the inter-related nature of growth trajectories of each modality [13].

3   Analysis of Early Brain Growth

Data: This dataset consists of 70 healthy children, with 40 male and 30 females. Generally, subjects were scanned at 3 time points at approximately 6 months, 1 year, and 2 years of age, however, some subjects (19) have 2 observations. MR acquisition was performed using a 3-T Siemens Tim Trio scanner with a 12-channel head coil at multiple sites with protocol T1 magnetization-prepared rapid acquisition gradient-echo (MPRAGE) scan T2 fast spin echo (FSE) scan. A LEGO phantom was scanned every month at all acquisition sites to correct for image quality issues and site-specific regional distortions. Additionally, two human phantoms were scanned once each year per scanner. Inter-site and intra-site stability was tested using these human phantoms across multiple sites [14].
Results: All subject images were processed by a pipeline including co-registration, tissue segmentation, and lobar parcellation as described in the Sect. 2. An example of a co-registered set of multimodal scans from a single subject is shown in Fig. 1, along with the corresponding segmentation and parcellation maps. Preprocessing was followed by calculation of intensity distributions and WIVID distribution overlap per lobe and timepoint for WM and GM tissue classes. The temporal series of WIVID measures was then modeled using the multilevel NLME model described in the previous section (see Fig. 1 middle and right).

To effectively model the dataset, joint multivariate modeling of WIVID using both T1 and T2 modalities was performed. Asymptote and delay were chosen
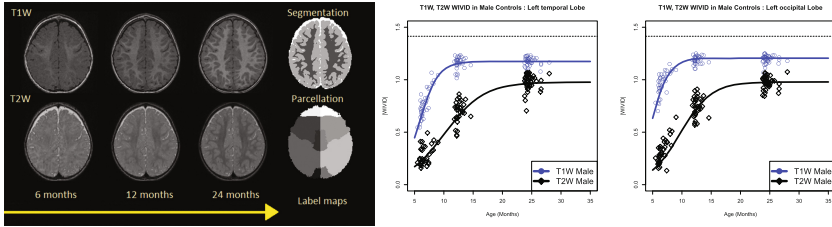
Fig. 1. Left: Processing framework illustrating co-registered multimodal T1W and T2W scans at 6, 12 and 24 months along with segmentation and lobe parcellation maps. Middle and right: Results from multilevel NLME modeling of contrast trajectories in males. Plots for T1W scans (blue) and T2W scans (black) are shown for the left temporal lobe and left occipital lobe.

to have random effects components in the model while a fixed effects component was associated with the rate of change. The plots illustrate that the change in contrast is highly asymptotic, and that trajectories and rate of change in different modalities are very different. The T1W WIVID contrast values increase sharply between 6 months and 1 year of age, after which they only have slow variation. In comparison, the T2W WIVID contrast values are initially much lower but continue to increase throughout the age range from 6 months until 2 years.

Figure 2 illustrates lobar patterns of maturation that proceed from anterior to posterior brain regions. Visualizations show the timing of the inflection point of the NLME fit per lobe regions, and only the T2 trajectories are used due the increased age range where changes are observable. The same pattern is also observable via delay and rate parameters from the NLME fit but tables are omitted due to space limitations. Most noticeably, while the occipital lobe has the lowest delay value indicating early maturation, frontal and temporal lobes have
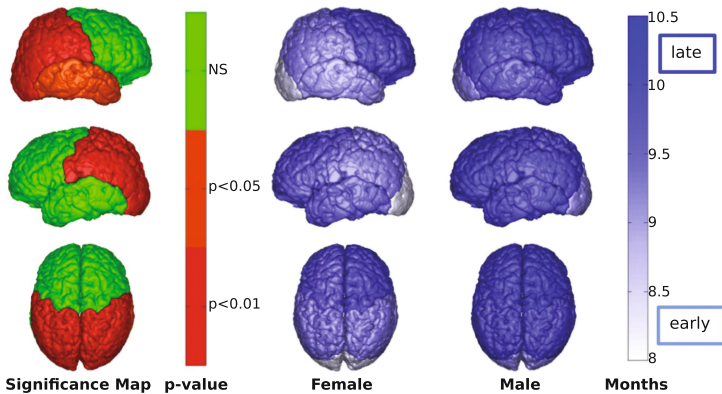

Fig. 2. Visualization of analysis of contrast trajectories. Left: P-values corresponding to the delay parameters (prior to correction for multiple comparisons). Delay parameters for female (middle) and male (right) subjects.
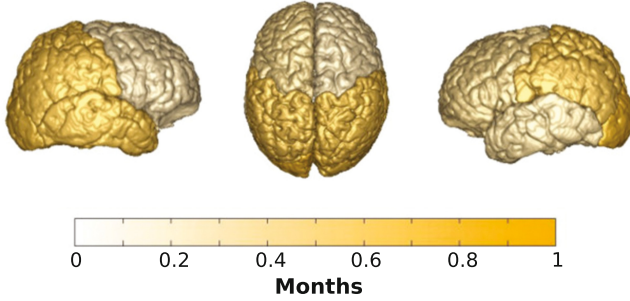
Maturation rate difference between male and female

Months

Fig. 3. Difference in delay parameter between male and female groups visualized across major brain lobes of the cerebral cortex.

the highest delay value corresponding to late maturation. The same spatial pattern is seen for female and male subjects, which corroborate common knowledge in pediatric radiology [2,15]. Most interesting is the differences in delay between female and male groups, where females show earlier maturation than male subjects. Timing differences are shown in Fig. 3. A qualitative interpretation reveals that sex differences are highest in regions which also mature earlier, i.e. in the occipital and parietal lobes. Regions with later development such as temporal and frontal lobes show smaller sex differences. It is important to note that these maturation patterns are measured at an age where there is very limited access to cognitive assessments of infant growth.

4   Discussion

This work characterizes spatiotemporal patterns of brain growth using intertissue contrast from longitudinal pediatric neuroimaging data of healthy subjects. Unlike most published work on early infant growth, contrast from multimodal MRI was used as a measure of longitudinal change. The distance measure between gray and white matter intensity distributions is invariant to scale and does not require normalization of MRI intensities which itself would represent a significant challenge. Patterns that are commonly mentioned in neuroimaging literature such as the posterior-to-anterior patterns of brain maturation in the major lobes of the cerebral cortex are quantified using parameters emerging from the NLME logistic fit. Differences shown in appearance change across different modalities have the potential to capture timing sequences of underlying neurobiological properties. The finding of male-female differences being more apparent in posterior brain regions indicate that such a method has potential to detect maturation delays in infants at risk for mental illness at an age where there are very limited other ways to assess development and growth. Improved understanding of developmental origins and timing is a declared goal of research in mental illness, and making use of image contrast in addition to volumetry,

shape, or diffusion measures may potentially add information not sufficiently studied before.

The variation of contrast with respect to nonlinear intensity distortions has not been fully examined. As a result, the effect of intensity inhomogeneities including bias distortions on contrast is not fully known. A prerequisite for proposed methodology is brain tissue segmentation at all time points, even at stages where there is very little or disappearing tissue contrast. We have applied a 4D segmentation scheme via the use of a subject-specific atlas, indicating that multiple time points are necessary for an infant to be segmented. Further progress on multi-modal segmentation at this age range may provide solutions. Finally, quantitative investigations into the actual biophysical processes that result in brain appearance change would help to get further insight into the nature and extent of contrast variations in the infant brain.

References

1. Serag, A., Aljabar, P., Counsell, S., Boardman, J., Hajnal, J.V., Rueckert, D.: Tracking developmental changes in subcortical structures of the preterm brain using multi-modal MRI. In: IEEE ISBI, pp. 349–352 (2011)
2. Rutherford, M.: MRI of the Neonatal Brain. WB Saunders Co, London (2002)
3. Prastawa, M., Sadeghi, N., Gilmore, J.H., Lin, W., Gerig, G.: A new framework for analyzing white matter maturation in early brain development. In: IEEE ISBI, pp. 97–100. IEEE (2010)
4. Jäger, F.: Normalization of Magnetic Resonance Images and its Application to the Diagnosis of the Scoliotic Spine, vol. 34. Logos Verlag Berlin GmbH, Berlin (2011)
5. Deoni, S.C., Mercure, E., Blasi, A., Gasston, D., Thomson, A., Johnson, M., Williams, S.C., Murphy, D.G.: Mapping infant brain myelination with magnetic resonance imaging. J. Neurosci. **31**(2), 784–791 (2011)
6. Ge, Y., Udupa, J.K., Nyul, L.G., Wei, L., Grossman, R.I.: Numerical tissue characterization in MS via standardization of the MR image intensity scale. J. Magn. Reson. Imaging **12**(5), 715–721 (2000)
7. Vardhan, A., Prastawa, M., Vachet, C., Piven, J., Gerig, G.: Characterizing growth patterns in longitudinal MRI using image contrast. In: SPIE Medical Imaging, p. 90340D (2014)
8. Shi, F., Fan, Y., Tang, S., Gilmore, J.H., Lin, W., Shen, D.: Neonatal brain image segmentation in longitudinal MRI studies. Neuroimage **49**(1), 391–400 (2010)
9. Joshi, S., Davis, B., Jomier, M., Gerig, G.: Unbiased diffeomorphic atlas construction for computational anatomy. NeuroImage **23**, S151–S160 (2004)
10. Van Leemput, K., Maes, F., Vandermeulen, D., Suetens, P.: Automated model-based tissue classification of MR images of the brain. IEEE Trans. Med. Imaging **18**(10), 897–908 (1999)
11. Kailath, T.: The divergence and Bhattacharyya distance measures in signal selection. IEEE Trans. Commun. Technol. **15**(1), 52–60 (1967)
12. Lindstrom, M.L., Bates, D.M.: Nonlinear mixed effects models for repeated measures data. Biometrics **46**(3), 673–687 (1990)

13. Vardhan, A., Prastawa, M., Sadeghi, N., Vachet, C., Piven, J., Gerig, G.: Joint longitudinal modeling of brain appearance in multimodal MRI for the characterization of early brain developmental processes. In: Durrleman, S., Fletcher, T., Gerig, G., Niethammer, M., Pennec, X. (eds.) STIA 2014. LNCS, vol. 8682, pp. 49–63. Springer, Cham (2015). doi:10.1007/978-3-319-14905-9_5

14. Gouttard, S., Styner, M., Prastawa, M., Piven, J., Gerig, G.: Assessment of reliability of multi-site neuroimaging via traveling phantom study. In: Metaxas, D., Axel, L., Fichtinger, G., Székely, G. (eds.) MICCAI 2008. LNCS, vol. 5242, pp. 263–270. Springer, Heidelberg (2008). doi:10.1007/978-3-540-85990-1_32

15. Barkovich, A.J.: Pediatric Neuroimaging. Lippincott Williams & Wilkins, Philadelphia (2005)